

Evaluation of MR Imaging Biomarkers of the Diffuse Infiltrative Phenotype in Orthotopic Brain Tumours

Jessica K. R. Boulton¹, Lara Perryman^{2,3}, Alexa Jury^{2,3}, Gary Box³, Paola Porcari^{1,4}, Sergey Popov^{2,3}, Suzanne A. Eccles³, Chris Jones^{2,3}, and Simon P. Robinson¹
¹CRUK and EPSRC Cancer Imaging Centre, The Institute of Cancer Research and Royal Marsden NHS Foundation Trust, Sutton, Surrey, United Kingdom, ²Division of Molecular Pathology, The Institute of Cancer Research, Sutton, Surrey, United Kingdom, ³CRUK Cancer Therapeutics Unit, The Institute of Cancer Research, Sutton, Surrey, United Kingdom, ⁴Physics Department, Sapienza University of Rome, Rome, Italy

Introduction

Despite recent treatment advances, high grade glioblastoma multiforme (GBM) remains a leading cause of tumour-related morbidity and mortality in children and adults. In diffuse infiltrative GBM, cells invade along the myelinated fibres in white matter tracts and obtain essential nutrients by co-opting existing vasculature. The blood brain barrier (BBB) remains intact in areas of infiltrative growth. Thus, not only is drug delivery limited in these areas, but also appropriate delineation of tumours using conventional Gd-DTPA enhanced MRI can be problematic, as extravasation of Gd-DTPA is precluded. Anti-VEGF treatment has been shown to restore the compromised BBB of neovascular regions, resulting in reduced tumour detectability in Gd-DTPA enhanced MRI [1]. Furthermore, such treatment strategies have been shown to promote GBM invasion [2]. Preclinical models that emulate diffuse brain tumours, in which to evaluate novel therapeutics, are limited. Therefore, we aimed to develop an invasive intracranial tumour model, and to use a multiparametric MRI approach encompassing native measurements and the combined use of quantitative Gd-DTPA and USPIO enhanced MRI to interrogate the detection of diffuse infiltrative tumour growth.

Methods

Cryopreserved, disaggregated cell preparations from paediatric GBM were implanted into the brains of female NCr nude mice (n=8) and tumour growth monitored using MRI. Luciferase-expressing MDA-MB-231 highly malignant human triple negative breast adenocarcinoma cells (5×10^3) were similarly implanted (n=6) and their establishment and growth monitored by bioluminescence imaging. MRI was performed on a Bruker 7T horizontal bore microimaging system, using a 3cm birdcage ¹H coil over a 2.5cm FOV. Both lateral tail veins were cannulated with heparinised 27G butterfly catheters for the administration of contrast agents. Axial T₂-weighted RARE images were acquired to monitor growth or localise established tumours. An echo-planar diffusion-weighted (EPI-DWI) sequence (T_R=3000ms, 6 b-values; b=40, 100, 200, 500, 700, 1000s/mm², 4 averages) was used to determine the apparent diffusion coefficient (ADC). Fluid attenuated inversion recovery (FLAIR) images were also acquired (RARE; T_R=18000ms, T_Eeff=35ms, T₁=2100ms, 4 averages). T₁-weighted RARE and inversion recovery (IR) true-FISP sequences were performed prior to, and following, administration of 0.1mmol/kg Gd-DTPA i.v. (Magnevist, Schering). Multi gradient-recalled echo (MGE) images were acquired prior to, and following, USPIO administration i.v. (150µmolFe/kg P904, Guerbet) [4]. Diffusion, IR-trueFISP and MGE data were fitted on a voxel-by-voxel basis using in-house software, providing maps of tumour spatial heterogeneity of ADC, ΔR_1 with Gd-DTPA and ΔR_2^* with USPIO, the latter used to synthesise maps of fractional blood volume (fBV, %). The median value of each parameter in each tumour was determined. Following MRI, brains were fixed in 10% formal saline for 24 hours, embedded in paraffin wax and H&E staining was performed to assess tumour extent and infiltration.

Results & Conclusions

Primary GBM xenografts (n=2) presented >4 months after implantation as hyperintense lesions on T₂-weighted images (Figure 1), but with less well defined borders than many tumours derived from immortalised cell lines. A corresponding hyperintense region was evident on FLAIR images, indicative of an invasive phenotype. FLAIR is adopted clinically to identify diffuse infiltrative areas of brain tumours, and now forms part of the updated response assessment criteria for high grade GBM [5]. No parenchymal enhancement was observed following Gd-DTPA administration, as exemplified in the ΔR_1 map in Figure 1, suggesting an intact BBB. Similarly, negligible signal change was observed in MGE images following USPIO administration. H&E staining revealed the tumour phenotype to be consistent with a grade III anaplastic diffuse astrocytoma, presenting as a hypercellular lesion with a diffuse growth pattern, poorly defined margins and comprised of pleomorphic astrocytic cells with elongated or angulated nuclei (arrows on high power image, Figure 1). No evidence of necrosis or microvascular proliferation was observed.

MDA-MB-231 tumours were well established at the time of MRI (~day 30), with a mean volume of $58 \pm 6 \text{mm}^3$. Tumours presented as heterogeneous hyperintense lesions on T₂-weighted images (Figure 2). ADC maps were heterogeneous (mean $782 \pm 26 \times 10^{-6} \text{cm}^2 \text{s}^{-1}$), with areas of high ADC correlating with the most hyperintense regions of the tumour in T₂-weighted images and areas of histologically confirmed oedema (closed head arrows on H&E images, Figure 2). Parenchymal enhancement following administration of Gd-DTPA was also spatially heterogeneous (ΔR_1 map, Figure 2), with a cohort mean ΔR_1 of $0.57 \pm 0.09 \text{s}^{-1}$. Regions of large ΔR_1 were distinct from the areas of high ADC, but correlated with the regions of high fBV (mean $7.3 \pm 0.5\%$, map not shown). Tumour extent was assessed from composite images of H&E stained sections; the tumours grew as partially well-circumscribed masses with substantial local invasion. Infiltration typically occurred along existing blood vessels, but also through the brain parenchyma; the infiltrative regions corresponded to regions of limited Gd-DTPA extravasation and low fBV.

We have shown that direct grafting of patient-derived GBM cells results in a clinically relevant, invasive phenotype, but these models take a long time to develop, have a low success rate, and cannot easily be monitored. The MDA-MB-231-luc tumour described represents an ideal model for further development of imaging biomarkers of the invasive phenotype for use in the evaluation of novel therapeutic agents. The use of native and dual contrast enhanced MRI will facilitate the assessment of different growth patterns, functional vascular phenotypes and allow for deeper interrogation of treatment response in orthotopic brain tumours. Response to anti-angiogenic agents, which pre-clinically have been shown to restore the blood brain barrier, and appear to resolve oedema in the clinic [6], will be a particularly interesting option. It may also be possible to evaluate any therapy-induced changes in invasion using this method.

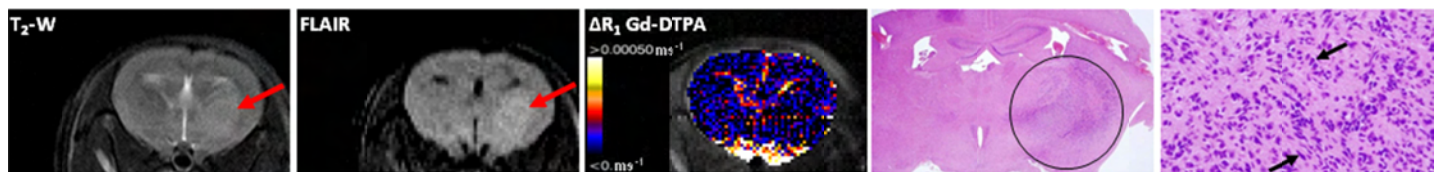


Figure 1. MRI and histology of a primary paediatric GBM xenograft in mouse brain. Hyperintense lesion evident on T₂-weighted and FLAIR images (red arrows). Tumour growth pattern shown to be diffuse by H&E staining (circle on whole brain image), cells with elongated or angulated nuclei indicated on x200 image.

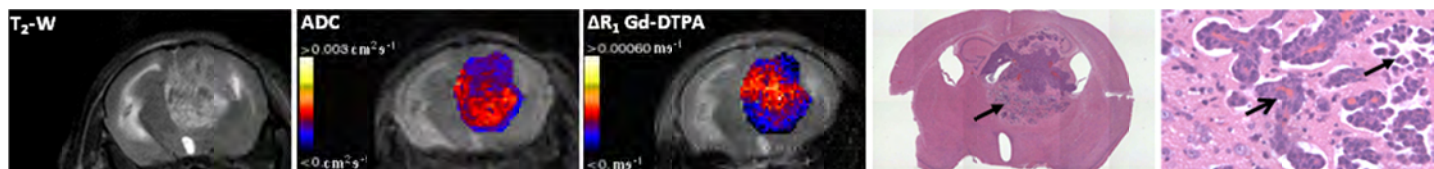


Figure 2. Multiparametric MRI of a representative MDA-MB-231 breast tumour xenograft in mouse brain with histological validation. Tumour heterogeneity evident in T₂-weighted images and parametric maps of ADC and ΔR_1 resulting from Gd-DTPA administration. H&E staining revealed tumour extent, invasion along blood vessels (open head arrow) and evidence of oedema (closed head arrows). H&E x200 magnification.

References. [1] Claes A *et al* (2008) *Int J Cancer* 122;1981-6. [2] DeGroot JF *et al* (2010) *Neuro Oncol* 12;233-42. [3] Lin N *et al* (2004) *J Clin Oncol* 22;3608-17. [4] Boulton JKR *et al* (2011) *Proc Intl Soc Mag Reson Med* 19. [5] Wen P *et al* (2010) *J Clin Oncol* 28;1963-72. [6] Batchelor TT *et al* (2007) *Cancer Cell* 11;83-95.

Acknowledgments. We acknowledge the support received for the CRUK and EPSRC Cancer Imaging Centre in association with the MRC and Department of Health (England) (grants C1060/A10334 and C16412/A6269) and NHS funding to the NIHR Biomedical Research Centre.